Development of a Virus Particle-Based Antibody-Dependent Cellular Phagocytosis (ADCP) Assay for HIV

Chitra Upadhyay[1*] and Priyanka Gadam Rao[1]

[1]Division of Infectious Diseases, Department of Medicine, Icahn School of Medicine at Mount Sinai, New York, New York, USA.

*** Correspondence:**
Corresponding Author
Chitra.Upadhyay@mssm.edu

Keywords: HIV, ADCP, Fc-mediated activity, THP-1 cells, virions, flow cytometry

3405 words, 6 figures.

Abstract (150 words)

Antibody-dependent cellular phagocytosis (ADCP) is an Fc-mediated effector function that contributes to the clearance of pathogens, including HIV. Conventional bead-based ADCP assays using recombinant Env proteins provide valuable insights but do not recapitulate the structural and antigenic complexity of intact virions, potentially limiting their physiological relevance. Here, we describe a virus particle-based ADCP assay that preserves the native conformation and glycosylation of the HIV envelope glycoprotein (Env), features critical for antibody recognition and Fcγ receptor engagement. The assay utilizes THP-1 monocyte-derived cells as effector cells and sucrose purified HIV-1 virions coupled with fluorescent beads, as targets. This platform enables sensitive and reproducible measurement of antibody-mediated phagocytosis in a biologically relevant context, facilitating accurate assessment of Fc effector functions across monoclonal and polyclonal antibody samples from multiple species. The approach addresses key limitations of traditional assays and provides a scalable tool for evaluating humoral immunity in HIV infection and vaccine studies.

Introduction

Broadly neutralizing antibodies (bNAbs) are a major focus of HIV vaccine and therapeutic research due to their demonstrated ability to prevent infection and suppress viraemia in both preclinical and clinical settings. In nonhuman primate (NHP) and humanized mouse models, passive administration of bNAbs has been shown to protect against simian-human immunodeficiency virus (SHIV) and HIV challenge respectively (1-7). Clinical trials, including the AMP studies, have further validated this approach, demonstrating up to 75% protection against bNAb-sensitive HIV-1 strains in humans (8). These findings highlight the central role of bNAbs as correlates of protection.

The predominant mechanism underlying bNAb-mediated protection is Fab-mediated neutralization, where antibodies block viral entry by targeting the conserved regions of the HIV-1 envelope glycoprotein (Env) (9, 10). However, accumulating evidence indicates that Fc-mediated effector functions such as antibody-dependent cellular phagocytosis (ADCP), antibody-dependent cellular cytotoxicity (ADCC), and complement activation, also contribute to antiviral efficacy, facilitating clearance of infected cells and virions (11-18). The interplay between Fab- and Fc-dependent mechanisms is increasingly recognized as critical for the breadth and durability of bNAb-mediated protection.

In the context of HIV-1, ADCP has been associated with reduced infection risk in NHP vaccine studies (19, 20) and in human clinical trials, including RV144 and HVTN 505, where ADCP activity correlated with decreased HIV-1 acquisition (11, 21). These findings highlight the need to better understand and quantify ADCP as a correlate of protective immunity. Several assay platforms have been developed to evaluate ADCP in the context of HIV. The most widely adopted approach utilizes beads coated with HIV Env proteins, which are opsonized by antibodies and subsequently internalized by monocytic cell lines such as THP-1 (22-27). This bead-based assay format is highly scalable and reproducible, enabling quantitative assessment of Fc-mediated phagocytic activity across diverse antibody specificities. Infected cell-based assays offer greater physiological relevance by presenting native trimeric Env on the surface of infected cells targets (28), but they are technically demanding and subject to variability in antigen density and cell viability (29-31). Despite their utility, both formats share a key limitation: they do not directly measure the phagocytosis of authentic HIV virions (31, 32). Bead-based systems using recombinant Env proteins (e.g., gp120, gp140, V3 or V1V2 proteins) (24-27) oversimplify Env presentation, omitting critical conformational and glycan features of the native trimer, and thus do not fully recapitulate the antigenic landscape of intact virions. Infected cell assays incorporate viral antigens in a more native context but do not capture particle-level clearance, and their technical complexity and variability limit their reproducibility and scalability for large studies. These limitations restrict our ability to fully evaluate how Fab and Fc mechanisms cooperate to mediate phagocytosis of HIV particles in a physiologically relevant context.

The aim of this study was to develop a virion-based ADCP assay that enables direct measurement of antibody-mediated phagocytosis of HIV virions. By coupling native HIV virions to fluorescent beads, this approach integrates the biological relevance of viral particles with the scalability and reproducibility of conventional bead-based platforms. The combination of physiologically relevant antigen presentation and high-throughput compatibility makes the virion-bead ADCP assay well-suited for vaccine evaluation, systems serology, and translational studies focused on identifying correlates of protective immunity. This platform supports robust functional profiling in both research and clinical settings.

Materials and Methods

Cell lines. The HEK293T/17 (293T) were obtained from the American Type Culture Collection (ATCC, Manassas, VA). The following reagent was obtained through the NIH HIV Reagent Program, Division of AIDS, NIAID, NIH: TZM-bl Cells, ARP-8129, contributed by Dr. John C. Kappes, Dr. Xiaoyun Wu, and Tranzyme Inc (33). For all experiments, HEK293T/17 cells (293T) were used to produce infectious HIV-1 viruses and the TZM.bl cell line was used to assay virus infectivity. TZM.bl cell line is derived from HeLa cells and is genetically modified to express high levels of CD4, CCR5 and CXCR4 and contains reporter cassettes of luciferase and β-galactosidase that are each expressed from an HIV-1 LTR. The 293T and TZM.bl cell lines were routinely sub-cultured every 3 to 4 days by trypsinization and were maintained in Dulbecco's Modified Eagle's Medium (DMEM) supplemented with 10% heat-inactivated fetal bovine serum (FBS), HEPES pH 7.4 (10 mM), L-glutamine (2 mM), penicillin (100 U/ml), and streptomycin (100 µg/ml) at 37°C in a humidified atmosphere with 5% CO2.

THP-1 cells are a human monocytic cell line commonly used in ADCP assays to model macrophage-mediated phagocytosis. THP-1 cells were purchased from ATCC and maintained in RPMI 1640 media (ATCC) containing 2 mM L-Glutamine (Gibco), 10% Fetal Bovine Serum (Sigma), 10 mM HEPES (Gibco), 55 µM beta-mercaptoethanol (Gibco), and 1X Penicillin/Streptomycin (Gibco). Cell culture densities were kept below 0.5×10^6 cells/ml to maintain consistent assay performance.

Plasmids. A full-length transmitted/founder (T/F) infectious molecular clone (IMC) of pREJO.c/2864 (REJO, ARP-11746) was obtained through the NIH HIV Reagent Program, Division of AIDS, NIAID, NIH, contributed by Dr. John Kappes and Dr. Christina Ochsenbauer (34). REJO is a tier 2, clade B, T/F isolate. The IMC of RHPA and QH0692 (tier 2, clade B, T/F) were kindly provided by Dr Benjamin Chen. The IMCs were generated by cloning the Env into a pNL4.3 backbone to construct pNL-RHPA and pNL-QH0692, respectively (35). The CMU06 IMC was generated similarly by cloning the Env into a pNL4.3 backbone to construct pNL-CMU06(35).

Antibodies. The following antibody reagents used in this study were obtained through the NIH AIDS Reagent Program, Division of AIDS, NIAID, NIH: Anti-HIV-1 gp120 monoclonal VRC01 from Dr. John Mascola (36); anti-HIV-1 gp120 monoclonal antibody NIH45-46 G54W, contributed by Dr. Pamela Bjorkman (37); anti-HIV-1 gp41 monoclonal 2F5 from Polymun Scientific (38); polyclonal HIV-Ig contributed by Dr. Luiz Barbosa. The V2i (830) and V3 (2219) and the irrelevant (non-HIV-1) anti-anthrax 3685 mAbs were obtained from the laboratory of Dr. Susan Zolla-Pazner (39-47). The mAb 3685 was used as a negative control. HIV-1 positive human plasma samples used were a gift from Dr Colleen Courtney (48). Mouse monoclonal antibodies and plasma samples were from vaccination experiments from our lab.

Virus production and purification. Infectious viruses were generated by transfecting 293T cells with pREJO, pNL-CMU06, pNL-RHPA and pNL-QH0692 plasmids using jetPEI transfection reagent (Polyplus, New York, NY)(49). Supernatants were harvested after 48 hours and clarified by centrifugation and 0.45µm filtration. Virus infectivity was assessed on TZM.bl cells as described(35, 49). Briefly, serial two-fold dilutions of virus stock in 10% DMEM were incubated with TZM.bl cells (in duplicates for each dilution) in half-area 96-well plates in the presence of DEAE-dextran (12.5 µg/ml) for 48 hours at 37°C. Virus infectivity was measured by β-galactosidase activity (Promega, Madison, WI). Virus stocks were concentrated (20X) by ultracentrifugation over 20% (w/v) sucrose in 1X phosphate buffered saline (PBS) at 25,000 RPM for 2 hours in an SW-28 swinging bucket rotor (Sorvall, Thermofisher Scientific). Supernatants were decanted and pellets dried briefly before resuspension in PBS. Inactivation of virions was carried out using Aldrithiol-2 (AT-2) (50, 51). Briefly,

111 125 ul of sucrose-purified virus was incubated with 0.5 mM AT-2 in DMSO for 2 hours at 37°C,
112 followed by centrifugation at 13,000 rpm for 2 hours. The supernatant was discarded, and the pellet re-
113 suspended in 125 ul PBS. Inactivation was confirmed by measuring infectivity in TZM.bl cells and
114 Env content was checked by Western blotting.

115 **Western blotting.** To quantify and monitor the expression of Env in each virus preparation
116 Western blot analyses were performed. The sucrose-purified virus particles were lysed, resolved by
117 SDS-PAGE on 4–20% tris-glycine gels (Bio-Rad, Hercules, CA), and blotted onto membranes, which
118 were then probed with antibodies. A cocktail of anti-human anti-gp120 MAbs (anti-V3: 391, 694, 2219,
119 2558; anti-C2: 841, 1006; anti-C5: 450, 670, 722; 1μg/ml each) was used to detect Env. MAb 91-5D
120 (1μg/ml) was used to detect Gag p24. Membranes were developed with Clarity Western ECL Substrate
121 (Bio-Rad, Hercules, CA) and imaged by iBright FL1500 Imaging System (Invitrogen, Carlsbad, CA).
122 Purified recombinant gp120 and p24 proteins were also loaded at a known concentration as controls
123 and quantification standards. Band intensities were quantified using the iBright Analysis Software
124 Version 5.0.1 (Invitrogen, Carlsbad, CA).

125 **Coupling of fluorescent beads to virions.** The coupling strategy used in this study is a standard
126 method widely used in the Luminex based multiplex immunoassays and is published previously(52-
127 55). Here we applied this approach for coupling the virus to the beads. Sucrose-purified, inactivated
128 virions were covalently coupled to carboxylate-modified microspheres (1.0 μm) using a two-step
129 carbodiimide reaction with the xMAP Ab Coupling (AbC) Kit according to manufacturers' instructions
130 (Luminex, Austin, TX). Carboxylated beads purchased from Thermo Fisher (cat# F8823), were
131 coupled to 125 μl of 20X concentrated virus preparations (~36.4×10^9 beads per reaction). Briefly, the
132 stock microspheres were vortexed and sonicated to resuspend and disperse the microspheres and 12 μl
133 was transferred to a tube containing 1200 ul of 1% BSA/1X PBS (per virus). The microspheres were
134 washed twice with 500 μl of activation buffer followed by vortexing and sonication after each step.
135 The microspheres were activated with 400 μL of activation buffer, 50 μL of 50 mg/ml Sulfo-NHS (N-
136 hydroxysulfosuccinimide), 50 μL of 40 mg/mL ethyl dimethylaminopropyl carbodiimide
137 hydrochloride (EDC) and incubated for 20 min at room temperature with end-to-end rotation. The
138 microspheres were washed three times in activation buffer, then incubated with AT-2 inactivated virus
139 in activation buffer for 2 hours at room temperature. We typically used a volume of 20X concentrated
140 virus that equals ~175ng total as measured by western blotting. The microspheres were subsequently
141 washed and resuspended in 1.2 mL of 0.1% BSA/PBS and stored at 4°C until ready to use.

142 **ADCP Assay Protocol.** The coupled microspheres (10 μl/well) were incubated with serial dilutions
143 of monoclonal antibodies or plasma for 2 hours at 37°C. Antibody opsonized virions coupled
144 microspheres were washed with 0.1% BSA/PBS twice to remove unbound antibodies. THP-1 cells
145 were added (200 μL/well) at a concentration of 1.25×10^5 cells/mL (2.5×10^4 cells/well) and incubated
146 with the immune complexed microspheres overnight for ~16 h at 37°C. Cells were then fixed with 4%
147 PFA and acquired on a Attune NxT flow cytometer. Data analysis was performed using FCS Express
148 7 Research Edition (De Novo Software). ADCP scores were calculated as follows: [(% microsphere
149 positive cells) x (geometric mean fluorescent intensity of the microsphere positive cells)/10,000].
150 Control wells including virion coupled beads alone, cells alone and virion coupled beads without Ab
151 and cells (no Ab control for background phagocytosis).

152 **Binding of mouse mAbs to virus-associated Env.** Binding of the virus coupled microspheres to
153 mouse mAbs were tested by flow cytometry (56) and by Luminex assay (27). <u>Flow cytometry virus</u>
154 <u>binding assay</u>: Virus-coupled microspheres were dispensed into 96-well plates (10 μl/well), blocked
155 with 3% BSA (100 μl, 30 min, 4°C), and centrifuged (2000 × g, 10 min). After discarding the
156 supernatant, microspheres were incubated with serially diluted mouse mAbs (30 min, 37°C), followed

157 by anti-mouse IgG biotin (1:500 in 0.1% BSA/PBS, 30 min, dark; Southern Biotech). After three PBS
158 washes, Streptavidin-PE (1:1000 in 0.1% BSA/PBS) was added (30 min), and microspheres were
159 resuspended in 200 µl of 0.5% paraformaldehyde. Flow cytometry (Attune NxT) was used to collect
160 >30,000 PE+ events. Data were analyzed in FCS-Express by gating FITC+ singlets and geometric
161 mean fluorescent intensity (MFI) values of PE+ beads representing anti-Env-stained virus particles
162 coupled to FITC microspheres were determined and plotted. MFI, as determined from microspheres
163 stained without primary antibodies was subtracted from all Env-mAb pairs. All mAbs were serially
164 diluted 3-fold starting at a concentration of 60 µg/ml. Luminex virus binding assay: Briefly, AT-2
165 inactivated virus was coupled to magnetic carboxylated fluorescent beads (Luminex Corp) using a
166 xMAP Antibody Coupling (AbC) Kit (Luminex). Mouse mAbs was tested at 60 µg/ml and IgG binding
167 to the beads was detected using anti-mouse IgG biotin (Southern Biotech) followed by Streptavidin-
168 PE. Samples were acquired on a Bio-Plex array reader (FlexMAP 3D, Luminex). Median fluorescence
169 intensities (MFI) were reported for each mAb.

170 **Statistical analysis.** Statistical analyses were performed as indicated in the figure legends with one
171 or two-way ANOVA using GraphPad Prism 10.6.0.

Results

Development of a virus particle-based ADCP assay. To establish a physiologically relevant platform for measuring Fc effector activity against HIV-1, we developed a virus particle-based antibody-dependent cellular phagocytosis (ADCP) assay. As shown in Figure 1A, sucrose-pelleted REJO virions were coupled to 1 μm yellow-green, fluorescent beads via a two-step carboxyl chemistry. These virion-coated beads were opsonized with antibody and incubated with THP-1 monocytic effector cells. After fixation, phagocytosis was quantified by flow cytometry using AlexaFluor488 fluorescence to detect bead uptake by THP-1 cells. Gating was performed on singlet THP-1 cells to exclude aggregates, and ADCP scores were calculated by multiplying the geometric mean fluorescence intensity (MFI) of bead-positive cells by the percentage of bead-positive cells, normalized to background.

Initially, we used RHPA, a T/F, clade B, tier 2, HIV-1 isolate and monoclonal antibodies (mAb) that recognize the conformational CD4bs (NIH45-46) epitope on Env. A non-HIV-1 mAb 3685 was used as a negative control. As shown in Figure 1B, the mAb NIH45-46 (red histogram) mediated robust phagocytic activity with an ADCP score of 1179.3, significantly higher than both the non-HIV-1 control mAb 3685 (green histogram; ADCP score = 667.3) and the background control with no antibody (gray histogram; ADCP score = 634.0). These results confirm the specificity and sensitivity of the assay for detecting Fc-mediated phagocytosis of antibody-opsonized HIV-1 virions.

Detection of ADCP activity by human monoclonal antibodies. We next applied the assay to evaluate the functional capacity of a panel of well-characterized human HIV-1 mAbs targeting diverse HIV-1 Env epitopes including the CD4 binding site (VRC01, NIH45-46), gp41 (2F5), V2 (830), and V3/linear epitopes (2219). Each mAb was tested across a range of concentrations using RHPA HIV-1 virion coupled to fluorescent beads and THP-1 monocytes. As shown in Figure 2A-B, some HIV-1-specific mAbs mediated dose-dependent phagocytosis, with NIH45-46 and 830 demonstrating the highest ADCP activity, followed by moderate responses from VRC01 and 2F5 (Fig 2A-C). As expected, the irrelevant anthrax-specific mAb 3685 showed no detectable activity, confirming assay specificity. The V3 mAb 2219 did not mediate detectable ADCP. Quantitative analysis of the area under the titration curves (AUC) from both experiments (Figure 2C) confirmed significant differences in potency across the panel, with NIH45-46 and 830 yielding the highest values. The irrelevant anthrax-specific mAb 3685 remained at baseline throughout, validating assay specificity.

Broad applicability across viral strains and antigens. To assess the generalizability of the ADCP assay across diverse HIV-1 strains and antigen formats, we tested the same mAb panel against virions from two additional isolates, CMU06 and REJO. With CMU06 (Figure 3A), mAbs 830 and 2219 mediated robust, dose-dependent ADCP, whereas NIH45-46, VRC01, 2F5, and the irrelevant control 3685 showed little or no activity. In contrast, with REJO virions (Figure 3B), 830 retained strong phagocytic activity while NIH45-46 showed only low activity; 2219, effective against CMU06, failed to mediate ADCP. These findings highlight strain-dependent differences in epitope accessibility, with CMU06 appearing more permissive than REJO, emphasizing the need to assess antibody function across multiple viral isolates rather than relying on a single strain.

We next compared ADCP activity against recombinant Env by testing the panel with REJO gp120 monomers coupled to beads (Figure 3C). The mAbs 830, 2219, and NIH45-46 mediated the strongest ADCP, while VRC01 exhibited weak activity only slightly above background. As expected, 2F5, which targets gp41, showed no activity. Overall, responses to gp120 were lower than those seen with intact virions, suggesting that the native conformation and membrane context of Env enhance Fcγ

216 receptor engagement. These results reinforce the added value of virion-based assays for functional
217 antibody profiling.

218 **Polyclonal HIV-1 infected sera mediate virion phagocytosis.** We next assessed whether the
219 assay developed could detect ADCP mediated by polyclonal antibodies. RHPA virion-coupled
220 fluorescent beads were incubated with heat-inactivated sera from HIV-1 infected individuals, as well
221 as with purified polyclonal immunoglobulin G (HIV-Ig) followed by THP-1 monocytes as phagocytic
222 effector cells. As shown in Figure 4A-B, sera from infected donors consistently mediated dose-
223 dependent ADCP activity, whereas HIV-1 negative sera (Neg) showed minimal activity. Quantitative
224 analysis of the area under the titration curves (AUC) confirmed significant higher ADCP activity in
225 HIV-1 infected sera compared to negative control (Figure 4C). These findings demonstrate that
226 naturally elicited polyclonal antibodies in chronic HIV-1 infection can direct Fc-mediated clearance of
227 virions and validate the sensitivity and biological relevance of the virion-based ADCP assay for
228 profiling humoral immunity.

229 **Extension of the assay to mouse monoclonal antibodies.** To expand the utility of the ADCP
230 assay to preclinical models, we tested murine (mu) Env-specific mAbs against RHPA and QH0692
231 virion-coupled beads. RHPA virions from two independent preparations (Prep 1 and Prep 2) and
232 QH0692 virions were coupled to fluorescent beads, opsonized with mouse mAbs, and incubated with
233 THP-1 monocytes. As shown in Figure 5A-B, mu-MAb1 and mu-MAb3 mediated dose-dependent
234 ADCP activity against RHPA virions, with consistent results across both virus preparations. The
235 irrelevant control antibody mu-MAb4 showed no activity, and specificity was further confirmed by the
236 Fc-impaired mu-MAb1 LALA variant, which failed to mediate ADCP (57-59). The assay also
237 performed well with QH0692 virions (Figure 5C), where Env-specific mAbs again showed strong
238 phagocytic responses, while mu-MAb4 remained negative. Collectively, these results demonstrate that
239 the assay is compatible with murine antibodies, reproducible across virus preparations, and effective
240 with distinct HIV-1 isolates, supporting its utility for evaluating antibody responses in animal models
241 of HIV-1 vaccination or infection.

242 Figure 5D and 5E confirm that all tested mouse mAbs were capable of binding to virus-coupled
243 microspheres. Using a previously published flow cytometry-based virus binding assay (56), we
244 observed that all mouse mAbs bound RHPA virions at levels above the negative control (Figure 5D).
245 Similarly, the Luminex assay (27) showed consistent binding profiles across the same set of mAbs
246 (Figure 5E). These results validate the specificity of the antibodies and confirm that binding is
247 detectable across both platforms. Importantly, while all mouse mAbs demonstrated binding to virions,
248 only mu-MAb1 and mu-MAb3 mediated ADCP. Binding assay also validated the loss of ADCP
249 activity by the mutant mu-MAb1-LALA. This distinction underscores the critical role of Fc-effector
250 function in driving phagocytosis and highlights the value of combining binding and functional assays
251 to comprehensively characterize antibody responses.

252 **Detection of vaccine-elicited ADCP activity in mouse sera.** To evaluate the applicability of
253 the virion-based ADCP assay in a vaccination setting, sera from mice co-immunized with HIV-1 gp120
254 DNA and protein were tested. Serially diluted sera were incubated with REJO virions or REJO gp120
255 proteins coupled with fluorescent beads, followed by THP-1 phagocytic cells. Vaccinated sera
256 mediated dose-dependent phagocytosis of both virion- and gp120-coupled beads, whereas sera from
257 unimmunized controls (normal mouse serum, NMS) showed no activity (Fig 6A-B). Notably, the
258 magnitude of ADCP was higher with gp120-coated beads, nearly two-fold greater in animal M117 and
259 M120 compared to the virion-coated beads (Fig 6C). Although these results may appear to indicate
260 stronger antibody responses, they are confounded by the use of monomeric gp120, which lacks the

261 native trimeric architecture, membrane association, and extensive glycan shield characteristic of intact
262 HIV virions. The non-native epitopes are exposed on the monomeric gp120 allowing increased
263 antibody accessibility, thereby inflating measured ADCP activity relative to assays employing
264 physiologically relevant viral particles. By contrast, the virion-based assay preserves native antigenic
265 features, offering a more physiologically relevant measure of vaccine-elicited ADCP. These findings
266 underscore the importance of intact virions for functional antibody profiling and highlight the potential
267 of this platform as a robust tool in preclinical vaccine studies.

268

Discussion

Fc-mediated effector functions of antibodies, including ADCP, are increasingly recognized as important contributors to protective immunity against HIV, complementing Fab-mediated neutralization. However, current ADCP assays have notable limitations. While bead-based assays using recombinant Env proteins offer scalability and reproducibility, they fall short in mimicking the structural and glycan complexity of the native Env trimer found on HIV virions (22, 23). In contrast, infected cell-based assays provide more physiologically relevant antigen presentation but exhibit variability in antigen density and are difficult to standardize for broader applications (28).

To address these challenges, we developed a virion-based ADCP assay by coupling intact HIV-1 particles to fluorescent beads. This format retains critical conformational and glycosylation determinants of Env that govern antibody recognition and Fcγ receptor engagement, while remaining compatible with high-throughput flow cytometry. Importantly, it avoids the biosafety concerns and variability associated with assays that use free virus assays (32), offering a biologically relevant and scalable alternative. We employed THP-1 monocytes as effector cells due to their standardized and scalable nature. While they do not fully recapitulate the diversity of Fcγ receptor expression found in primary monocytes, macrophages, and dendritic cells, their cross-reactivity with IgG from multiple species enabled robust assessment of murine and rabbit antibodies alongside human IgG (24, 26, 60, 61). Future studies should extend validation to primary myeloid cells and additional viral clades to further strengthen its translational relevance.

Our findings contrast with those of Gach et al., who reported that HIV-1 virions are largely resistant to ADCP, even in the presence of potent HIV-specific antibodies (32). Their study used multiple effector cell types including THP-1 cells, U937 cells, and primary monocytes, but observed minimal ADCP activity. This inefficiency was attributed to the low density of envelope trimers on the virion surface, which limits effective Fcγ receptor engagement. In our study, we used virions equivalent to ~175ng Env per coupling reaction, a relatively low amount that likely does not increase antigen density compared to free virions. However, the bead-coupling strategy may have improved the spatial organization and presentation of Env on the particle surface, facilitating more consistent antibody engagement and downstream phagocytic signaling. This difference in antigen format, rather than antigen quantity, may have contributed to the robust ADCP activity observed in our assay. Importantly, we detected strong phagocytic responses mediated by both broadly neutralizing and non-neutralizing antibodies, as well as polyclonal sera from HIV-infected individuals and vaccinated mice, underscoring the sensitivity and versatility of the platform.

A key observation was the difference between gp120-coated beads and virion-based targets. For example, the V3-specific mAb 2219 displayed activity with gp120 beads but not with REJO virions, likely due to the exposure of non-native epitopes on recombinant proteins. On native HIV-1 particles, the V3 loop is typically masked by the trimeric envelope structure and extensive glycan shield, maintaining a closed conformation that restricts antibody binding (56, 62-64). This conformational masking likely rendered the 2219 epitope inaccessible on virions, explaining the absence of ADCP activity. These findings emphasize the importance of physiologically relevant antigen presentations in ADCP assays to accurately assess antibody function and highlight the limitations of bead-based systems employing recombinant proteins.

Overall, the virion-based ADCP assay provides a scalable, reproducible, and biologically relevant platform that bridges the gap between simplified bead systems and complex infected-cell assays. By enabling direct measurement of antibody-mediated phagocytosis of authentic HIV particles,

313 it offers a powerful tool for identifying correlates of protection, benchmarking therapeutic antibodies,
314 and evaluating vaccine-induced responses. Beyond HIV, this strategy is readily adaptable to other
315 enveloped viruses, including influenza, SARS-CoV-2, and filoviruses, where Fc effector functions play
316 critical roles in immunity (65).

317 **Figure Legends**

318 **Figure 1**. **ADCP Assay for Detecting Phagocytosis of Antibody-Opsonized HIV-1 Virions.**
319 **(A)** Schematic overview of the assay. Sucrose pelleted REJO virions were carboxyl-coupled to 1 μm
320 yellow-green beads. Virion-coupled bead were then incubated with HIV-1 envelope-specific mAb,
321 washed, incubated with human THP-1 monocytes, fixed, and analyzed by flow cytometry. **(B)** Gates
322 were drawn on singlet THP-1 cells, and phagocytic scores were calculated from data on the
323 AlexaFluor488 fluorescence channel to quantify envelope-specific ADCP. Histograms indicate results
324 with 5 μg/ml positive (NIH45-46; red) and negative control (3685-non-HIV-1; green)
325 mAbs. Background phagocytosis (Bk) of virion-couple beads with no Ab is shown in gray.

326 **Figure 2**. **ADCP assay for detection of phagocytosis of human antibody opsonized virions.** Sucrose
327 pelleted RHPA virions were carboxyl-coupled to 1 μm yellow-green beads. Virion-coupled bead were
328 then incubated with HIV-1 envelope-specific mAbs, washed, incubated with human THP-1 monocytes,
329 fixed, and analyzed by flow cytometry. Virion coupled beads incubated with cells without Ab were
330 used as background and subtracted. An irrelevant non-HIV-1 mAb specific to anthrax (3685) was used
331 as negative control. **(A)** Experiment 1 and **(B)** Experiment 2. **(C)** Area under titration curve (AUC)
332 values were calculated from Fig 2A and 2B. Shading (gray) indicates the AUC range for the negative
333 control mAb 3685. Comparisons were made between 3685 versus HIV-1 specific mAbs. *, $p \leq 0.05$;
334 **, $p \leq 0.01$; ****, $p < 0.0001$ by 2-way ANOVA. $p > 0.05$ was left unmarked.

335 **Figure 3**. **Broad Applicability of the ADCP Assay Across HIV-1 Strains and Antigen Formats.**
336 Sucrose pelleted virions were carboxyl-coupled to 1 μm yellow-green beads. Virion-coupled bead were
337 then incubated with HIV-1 envelope-specific mAb,s washed, incubated with human THP-1 monocytes,
338 fixed, and analyzed by flow cytometry. ADCP with **(A)** CMU06 virions, **(B)** REJO virions and **(C)**
339 Rejo gp120. Virion coupled beads incubated with cells without Ab were used as background and
340 subtracted. An irrelevant non-HIV-1 mAb specific to anthrax (3685) was used as negative control.
341 Comparisons were made between 3685 versus HIV-1 specific mAbs. *, $p \leq 0.05$; **, $p \leq 0.01$; ****,
342 $p \leq 0.0001$ by 2-way ANOVA. $p > 0.05$ was left unmarked.

343 **Figure 4**. **ADCP assay to measure phagocytosis of HIV-1 virions opsonized with polyclonal**
344 **antibodies from infected individuals.** Sucrose pelleted RHPA virions were carboxyl-coupled to 1 μm
345 yellow-green beads. The virion-coupled bead were incubated with heat-inactivated sera from HIV-1
346 infected individuals and polyclonal IgG (HIV-Ig), washed, then incubated with human THP-1
347 monocytes. After fixation samples were analyzed by flow cytometry. Virion coupled beads incubated
348 with cells in the absence of Ab served as background and were subtracted. Sera from healthy individual
349 (Neg) was used as negative control. **(A)** Experiment 1 and **(B)** Experiment 2. **(C)** Area under titration
350 curve (AUC) values were calculated from panel A and B. Gray shading indicates the AUC range for
351 the negative control polyclonal antibody (Neg). Comparisons were made between Neg versus HIV-1
352 specific antibodies. *, $p \leq 0.05$; **, $p \leq 0.01$; ***, $p \leq 0.0001$ by ANOVA. $p > 0.05$ was left unmarked.

353 **Figure 5**. **ADCP assay for detection of phagocytosis of mouse antibody opsonized virions.** Sucrose
354 pelleted RHPA virions were carboxyl-coupled to 1 μm yellow-green beads. Virion-coupled bead were
355 then incubated with HIV-1 envelope-specific mouse mAb, washed, incubated with human THP-1
356 monocytes, fixed, and analyzed by flow cytometry. RHPA viruses from two different transfections are
357 tested **(A)** Prep 1, **(B)** Prep 2. **(C)** Another T/F isolate QH0692 was tested similarly. Non-HIV- mouse
358 mAb mu-MAb4 was included as negative control. Virion coupled beads incubated with cells without
359 Ab were used as background and subtracted. Comparisons were made between mu-MAb4 versus HIV-

1 specific mouse mAbs. **, $p \leq 0.01$; *** $p \leq 0.001$; ****, $p \leq 0.0001$ by 2-way ANOVA. $p > 0.05$ was left unmarked.

Figure 5. ADCP and binding assays to evaluate mouse monoclonal antibody responses to HIV-1 virions. Sucrose pelleted RHPA virions were carboxyl-coupled to 1 µm yellow-green beads. Virion-coupled bead were then incubated with HIV-1 envelope-specific mouse mAb, washed, incubated with human THP-1 monocytes, fixed, and analyzed by flow cytometry. RHPA viruses from two different transfections are tested **(A)** Prep 1 **(B)** Prep 2). **(C)** Another T/F isolate QH0692 was tested similarly. Non-HIV- mouse mAb mu-MAb4 was included as negative control. Virion coupled beads incubated with cells without Ab were used as background and subtracted. (D) RHPA coupled beads were tested for binding to mouse mAbs by **(D)** flow cytometry **(E)** Luminex assay. Comparisons were made between mu-MAb4 versus HIV-1 specific mouse mAbs. *, $p < 0.05$; **, $p < 0.01$; *** $p < 0.001$; ****, $p < 0.0001$ by ANOVA. $p > 0.05$ was left unmarked.

Figure 6. A**ntibody-dependent cellular phagocytosis (ADCP) mediated by sera from immunized mice against REJO HIV-1 virions and gp120.** Sera from mice co-immunized with HIV-1 gp120 DNA + protein were tested for their ability to mediate ADCP using phagocytic THP-1 cells and fluorescent beads coated with **(A)** REJO virions and **(B)** REJO gp120. The ADCP scores were calculated by multiplying the geometric mean fluorescence intensity (MFI) of the bead-positive cells by the percentage of bead-positive cells. This value is then divided by 1,000. Background value as determined based on ADCP scores of cells and beads was used to set the background and subtracted. NMS is negative mouse sera for negative control. **(C)** Area under titration curve (AUC) values were calculated from panel A and B. Comparisons were made between NMS versus sera from HIV-1 immunized mice. **, $p \leq 0.01$; ****, $p \leq 0.0001$ by ANOVA. $p > 0.05$ was left unmarked.

Conflict of Interest

The authors declare that the research was conducted in the absence of any commercial or financial relationships that could be construed as a potential conflict of interest.

Author Contributions

CU conceived and designed the study. PR performed the experiments. CU and PR analyzed the data. CU wrote the original manuscript. CU and PR read and approved the final manuscript.

Funding

This work was supported by [NIH], grant number [AI140909 and AI179427] to CU.

Acknowledgments

The authors would like to thank Dr. Susan Zolla-Pazner and Ms. Xiaomei Liu for providing HIV-1-specific mAbs.

Data Availability Statement

The datasets generated for this study are available on request to the corresponding author.

396 **Reference**

397 1. Hessell AJ, Hangartner L, Hunter M, Havenith CEG, Beurskens FJ, Bakker JM, Lanigan
398 CMS, Landucci G, Forthal DN, Parren PWHI, Marx PA, Burton DR. 2007. Fc receptor but
399 not complement binding is important in antibody protection against HIV. Nature 449:101-
400 104.

401 2. Julg B, Sok D, Schmidt SD, Abbink P, Newman RM, Broge T, Linde C, Nkolola J, Le K, Su
402 D, Torabi J, Pack M, Pegu A, Allen TM, Mascola JR, Burton DR, Barouch DH. 2017.
403 Protective efficacy of broadly neutralizing antibodies with incomplete neutralization activity
404 against simian-human immunodeficiency virus in rhesus monkeys. Journal of Virology 91.

405 3. Ko SY, Pegu A, Rudicell RS, Yang ZY, Joyce MG, Chen X, Wang K, Bao S, Kraemer TD,
406 Rath T, Zeng M, Schmidt SD, Todd JP, Penzak SR, Saunders KO, Nason MC, Haase AT,
407 Rao SS, Blumberg RS, Mascola JR, Nabel GJ. 2014. Enhanced neonatal Fc receptor function
408 improves protection against primate SHIV infection. Nature 514:642-5.

409 4. Parren PWHI, Marx PA, Hessell AJ, Luckay A, Harouse J, Cheng-Mayer C, Moore JP,
410 Burton DR. 2001. Antibody protects macaques against vaginal challenge with a pathogenic
411 R5 simian/human immunodeficiency virus at serum levels giving complete neutralization in
412 vitro. Journal of Virology 75:8340-8347.

413 5. Pegu A, Yang ZY, Boyington JC, Wu L, Ko SY, Schmidt SD, McKee K, Kong WP, Shi W,
414 Chen X, Todd JP, Letvin NL, Huang J, Nason MC, Hoxie JA, Kwong PD, Connors M, Rao
415 SS, Mascola JR, Nabel GJ. 2014. Neutralizing antibodies to HIV-1 envelope protect more
416 effectively in vivo than those to the CD4 receptor. Sci Transl Med 6:243ra88.

417 6. Shingai M, Donau OK, Plishka RJ, Buckler-White A, Mascola JR, Nabel GJ, Nason MC,
418 Montefiori D, Moldt B, Poignard P, Diskin R, Bjorkman PJ, Eckhaus MA, Klein F, Mouquet
419 H, Lorenzi JCC, Gazumyan A, Burton DR, Nussenzweig MC, Martin MA, Nishimura Y.
420 2014. Passive transfer of modest titers of potent and broadly neutralizing anti-HIV
421 monoclonal antibodies block SHIV infection in macaques. Journal of Experimental Medicine
422 211:2061-2074.

423 7. Stephenson KE, Wagh K, Korber B, Barouch DH. 2020. Vaccines and Broadly Neutralizing
424 Antibodies for HIV-1 Prevention. Annu Rev Immunol 38:673-703.

425 8. Corey L, Gilbert PB, Juraska M, Montefiori DC, Morris L, Karuna ST, Edupuganti S, Mgodi
426 NM, deCamp AC, Rudnicki E, Huang Y, Gonzales P, Cabello R, Orrell C, Lama JR, Laher F,
427 Lazarus EM, Sanchez J, Frank I, Hinojosa J, Sobieszczyk ME, Marshall KE, Mukwekwerere
428 PG, Makhema J, Baden LR, Mullins JI, Williamson C, Hural J, McElrath MJ, Bentley C,
429 Takuva S, Gomez Lorenzo MM, Burns DN, Espy N, Randhawa AK, Kochar N, Piwowar-
430 Manning E, Donnell DJ, Sista N, Andrew P, Kublin JG, Gray G, Ledgerwood JE, Mascola
431 JR, Cohen MS, Hvtn H, Teams HHS. 2021. Two Randomized Trials of Neutralizing
432 Antibodies to Prevent HIV-1 Acquisition. N Engl J Med 384:1003-1014.

433 9. Gilbert PB, Huang Y, deCamp AC, Karuna S, Zhang Y, Magaret CA, Giorgi EE, Korber B,
434 Edlefsen PT, Rossenkhan R, Juraska M, Rudnicki E, Kochar N, Huang Y, Carpp LN,
435 Barouch DH, Mkhize NN, Hermanus T, Kgagudi P, Bekker V, Kaldine H, Mapengo RE,
436 Eaton A, Domin E, West C, Feng W, Tang H, Seaton KE, Heptinstall J, Brackett C, Chiong
437 K, Tomaras GD, Andrew P, Mayer BT, Reeves DB, Sobieszczyk ME, Garrett N, Sanchez J,
438 Gay C, Makhema J, Williamson C, Mullins JI, Hural J, Cohen MS, Corey L, Montefiori DC,

439 Morris L. 2022. Neutralization titer biomarker for antibody-mediated prevention of HIV-1
440 acquisition. Nature Medicine 28:1924-1932.

441 10. Pegu A, Borate B, Huang Y, Pauthner MG, Hessell AJ, Julg B, Doria-Rose NA, Schmidt SD,
442 Carpp LN, Cully MD, Chen X, Shaw GM, Barouch DH, Haigwood NL, Corey L, Burton DR,
443 Roederer M, Gilbert PB, Mascola JR, Huang Y. 2019. A Meta-analysis of Passive
444 Immunization Studies Shows that Serum-Neutralizing Antibody Titer Associates with
445 Protection against SHIV Challenge. Cell Host and Microbe 26:336-346.e3.

446 11. Chung AW, Ghebremichael M, Robinson H, Brown E, Choi I, Lane S, Dugast AS, Schoen
447 MK, Rolland M, Suscovich TJ, Mahan AE, Liao L, Streeck H, Andrews C, Rerks-Ngarm S,
448 Nitayaphan S, de Souza MS, Kaewkungwal J, Pitisuttithum P, Francis D, Michael NL, Kim
449 JH, Bailey-Kellogg C, Ackerman ME, Alter G. 2014. Polyfunctional Fc-effector profiles
450 mediated by IgG subclass selection distinguish RV144 and VAX003 vaccines. Sci Transl
451 Med 6:228ra38.

452 12. Hessell AJ, Hangartner L, Hunter M, Havenith CE, Beurskens FJ, Bakker JM, Lanigan CM,
453 Landucci G, Forthal DN, Parren PW, Marx PA, Burton DR. 2007. Fc receptor but not
454 complement binding is important in antibody protection against HIV. Nature 449:101-4.

455 13. Berendam SJ, Styles TM, Morgan-Asiedu PK, Tenney D, Kumar A, Obregon-Perko V, Bar
456 KJ, Saunders KO, Santra S, De Paris K, Tomaras GD, Chahroudi A, Permar SR, Amara RR,
457 Fouda GG. 2021. Systematic Assessment of Antiviral Potency, Breadth, and Synergy of
458 Triple Broadly Neutralizing Antibody Combinations against Simian-Human
459 Immunodeficiency Viruses. J Virol 95.

460 14. Schriek AI, Falck D, Wuhrer M, Kootstra NA, van Gils MJ, de Taeye SW. 2024. Functional
461 comparison of Fc-engineering strategies to improve anti-HIV-1 antibody effector functions.
462 Antiviral Res 231:106015.

463 15. Richardson SI, Chung AW, Natarajan H, Mabvakure B, Mkhize NN, Garrett N, Abdool
464 Karim S, Moore PL, Ackerman ME, Alter G, Morris L. 2018. HIV-specific Fc effector
465 function early in infection predicts the development of broadly neutralizing antibodies. PLoS
466 Pathog 14:e1006987.

467 16. Phelps M, Balazs AB. 2021. Contribution to HIV Prevention and Treatment by Antibody-
468 Mediated Effector Function and Advances in Broadly Neutralizing Antibody Delivery by
469 Vectored Immunoprophylaxis. Front Immunol 12:734304.

470 17. Richard J, Prevost J, Alsahafi N, Ding S, Finzi A. 2018. Impact of HIV-1 Envelope
471 Conformation on ADCC Responses. Trends Microbiol 26:253-265.

472 18. Dugast AS, Tonelli A, Berger CT, Ackerman ME, Sciaranghella G, Liu Q, Sips M, Toth I,
473 Piechocka-Trocha A, Ghebremichael M, Alter G. 2011. Decreased Fc receptor expression on
474 innate immune cells is associated with impaired antibody-mediated cellular phagocytic
475 activity in chronically HIV-1 infected individuals. Virology 415:160-7.

476 19. Barouch DH, Stephenson KE, Borducchi EN, Smith K, Stanley K, McNally AG, Liu J,
477 Abbink P, Maxfield LF, Seaman MS, Dugast AS, Alter G, Ferguson M, Li W, Earl PL, Moss
478 B, Giorgi EE, Szinger JJ, Eller LA, Billings EA, Rao M, Tovanabutra S, Sanders-Buell E,
479 Weijtens M, Pau MG, Schuitemaker H, Robb ML, Kim JH, Korber BT, Michael NL. 2013.
480 Protective efficacy of a global HIV-1 mosaic vaccine against heterologous SHIV challenges
481 in rhesus monkeys. Cell 155:531-9.

482 20. Barouch DH, Alter G, Broge T, Linde C, Ackerman ME, Brown EP, Borducchi EN, Smith
483 KM, Nkolola JP, Liu J, Shields J, Parenteau L, Whitney JB, Abbink P, Ng'ang'a DM, Seaman
484 MS, Lavine CL, Perry JR, Li W, Colantonio AD, Lewis MG, Chen B, Wenschuh H, Reimer
485 U, Piatak M, Lifson JD, Handley SA, Virgin HW, Koutsoukos M, Lorin C, Voss G, Weijtens
486 M, Pau MG, Schuitemaker H. 2015. Protective efficacy of adenovirus/protein vaccines
487 against SIV challenges in rhesus monkeys. Science 349:320-4.

488 21. Neidich SD, Fong Y, Li SS, Geraghty DE, Williamson BD, Young WC, Goodman D, Seaton
489 KE, Shen X, Sawant S, Zhang L, deCamp AC, Blette BS, Shao M, Yates NL, Feely F, Pyo
490 CW, Ferrari G, Team H, Frank I, Karuna ST, Swann EM, Mascola JR, Graham BS, Hammer
491 SM, Sobieszczyk ME, Corey L, Janes HE, McElrath MJ, Gottardo R, Gilbert PB, Tomaras
492 GD. 2019. Antibody Fc effector functions and IgG3 associate with decreased HIV-1 risk. J
493 Clin Invest 129:4838-4849.

494 22. Ackerman ME, Moldt B, Wyatt RT, Dugast AS, McAndrew E, Tsoukas S, Jost S, Berger CT,
495 Sciaranghella G, Liu Q, Irvine DJ, Burton DR, Alter G. 2011. A robust, high-throughput
496 assay to determine the phagocytic activity of clinical antibody samples. J Immunol Methods
497 366:8-19.

498 23. Tay MZ, Liu P, Williams LD, McRaven MD, Sawant S, Gurley TC, Xu TT, Dennison SM,
499 Liao HX, Chenine AL, Alam SM, Moody MA, Hope TJ, Haynes BF, Tomaras GD. 2016.
500 Antibody-Mediated Internalization of Infectious HIV-1 Virions Differs among Antibody
501 Isotypes and Subclasses. PLoS Pathog 12:e1005817.

502 24. Hioe CE, Kumar R, Upadhyay C, Jan M, Fox A, Itri V, Peachman KK, Rao M, Liu L, Lo NC,
503 Tuen M, Jiang X, Kong XP, Zolla-Pazner S. 2018. Modulation of Antibody Responses to the
504 V1V2 and V3 Regions of HIV-1 Envelope by Immune Complex Vaccines. Front Immunol
505 9:2441.

506 25. Hioe CE, Li G, Liu X, Tsahouridis O, He X, Funaki M, Klingler J, Tang AF, Feyznezhad R,
507 Heindel DW, Wang XH, Spencer DA, Hu G, Satija N, Prevost J, Finzi A, Hessell AJ, Wang
508 S, Lu S, Chen BK, Zolla-Pazner S, Upadhyay C, Alvarez R, Su L. 2022. Non-neutralizing
509 antibodies targeting the immunogenic regions of HIV-1 envelope reduce mucosal infection
510 and virus burden in humanized mice. PLoS Pathog 18:e1010183.

511 26. Hioe CE, Liu X, Banin AN, Heindel DW, Klingler J, Rao PG, Luo CC, Jiang X, Pandey S,
512 Ordonez T, Barnette P, Totrov M, Zhu J, Nadas A, Zolla-Pazner S, Upadhyay C, Shen X,
513 Kong XP, Hessell AJ. 2023. Vaccination with immune complexes modulates the elicitation of
514 functional antibodies against HIV-1. Front Immunol 14:1271686.

515 27. Upadhyay C, Rao P, Behzadi MA, Feyznezhad R, Lambert GS, Kumar R, Kumar M, Yang
516 W, Jiang X, Luo CC, Nadas A, Arthos J, Kong XP, Zhang H, Hioe CE, Duty JA. 2024. Signal
517 peptide exchange alters HIV-1 envelope antigenicity and immunogenicity. Front Immunol
518 15:1476924.

519 28. Bournazos S, Klein F, Pietzsch J, Seaman MS, Nussenzweig MC, Ravetch JV. 2014. Broadly
520 neutralizing anti-HIV-1 antibodies require Fc effector functions for in vivo activity. Cell
521 158:1243-1253.

522 29. Nagel L, Kant S, Leeks C, Routy JP, Tremblay C, Thomas R, Szabo J, Cote P, Trottier B,
523 LeBlanc R, Rouleau D, Dupuy FP, Bernard NF, investigators in Montreal Primary HIVIc.
524 2021. Evolution of Antibodies to Native Trimeric Envelope and Their Fc-Dependent
525 Functions in Untreated and Treated Primary HIV Infection. J Virol 95:e0162521.

526 30. Kant S, Zhang N, Barbe A, Routy JP, Tremblay C, Thomas R, Szabo J, Cote P, Trottier B,
527 LeBlanc R, Rouleau D, Harris M, Dupuy FP, Bernard NF. 2020. Polyfunctional Fc
528 Dependent Activity of Antibodies to Native Trimeric Envelope in HIV Elite Controllers.
529 Front Immunol 11:583820.

530 31. Snow BJ, Keles NK, Grunst MW, Janaka SK, Behrens RT, Evans DT. 2024. Potent broadly
531 neutralizing antibodies mediate efficient antibody-dependent phagocytosis of HIV-infected
532 cells. PLoS Pathog 20:e1012665.

533 32. Gach JS, Bouzin M, Wong MP, Chromikova V, Gorlani A, Yu KT, Sharma B, Gratton E,
534 Forthal DN. 2017. Human immunodeficiency virus type-1 (HIV-1) evades antibody-
535 dependent phagocytosis. PLoS Pathog 13:e1006793.

536 33. Platt EJ, Wehrly K, Kuhmann SE, Chesebro B, Kabat D. 1998. Effects of CCR5 and CD4 cell
537 surface concentrations on infections by macrophagetropic isolates of human
538 immunodeficiency virus type 1. J Virol 72:2855-64.

539 34. Ochsenbauer C, Edmonds TG, Ding H, Keele BF, Decker J, Salazar MG, Salazar-Gonzalez
540 JF, Shattock R, Haynes BF, Shaw GM, Hahn BH, Kappes JC. 2012. Generation of
541 transmitted/founder HIV-1 infectious molecular clones and characterization of their
542 replication capacity in CD4 T lymphocytes and monocyte-derived macrophages. J Virol
543 86:2715-28.

544 35. Upadhyay C, Feyznezhad R, Cao L, Chan KW, Liu K, Yang W, Zhang H, Yolitz J, Arthos J,
545 Nadas A, Kong XP, Zolla-Pazner S, Hioe CE. 2020. Signal peptide of HIV-1 envelope
546 modulates glycosylation impacting exposure of V1V2 and other epitopes. PLoS Pathog
547 16:e1009185.

548 36. Wu X, Yang ZY, Li Y, Hogerkorp CM, Schief WR, Seaman MS, Zhou T, Schmidt SD, Wu
549 L, Xu L, Longo NS, McKee K, O'Dell S, Louder MK, Wycuff DL, Feng Y, Nason M, Doria-
550 Rose N, Connors M, Kwong PD, Roederer M, Wyatt RT, Nabel GJ, Mascola JR. 2010.
551 Rational design of envelope identifies broadly neutralizing human monoclonal antibodies to
552 HIV-1. Science 329:856-61.

553 37. Diskin R, Scheid JF, Marcovecchio PM, West AP, Jr., Klein F, Gao H, Gnanapragasam PN,
554 Abadir A, Seaman MS, Nussenzweig MC, Bjorkman PJ. 2011. Increasing the potency and
555 breadth of an HIV antibody by using structure-based rational design. Science 334:1289-93.

556 38. Stiegler G, Kunert R, Purtscher M, Wolbank S, Voglauer R, Steindl F, Katinger H. 2001. A
557 potent cross-clade neutralizing human monoclonal antibody against a novel epitope on gp41
558 of human immunodeficiency virus type 1. AIDS Res Hum Retroviruses 17:1757-65.

559 39. Gorny MK, Moore JP, Conley AJ, Karwowska S, Sodroski J, Williams C, Burda S, Boots LJ,
560 Zolla-Pazner S. 1994. Human anti-V2 monoclonal antibody that neutralizes primary but not
561 laboratory isolates of human immunodeficiency virus type 1. J Virol 68:8312-20.

562 40. Gorny MK, Pan R, Williams C, Wang XH, Volsky B, O'Neal T, Spurrier B, Sampson JM, Li
563 L, Seaman MS, Kong XP, Zolla-Pazner S. 2012. Functional and immunochemical cross-
564 reactivity of V2-specific monoclonal antibodies from HIV-1-infected individuals. Virology
565 427:198-207.

566 41. Nyambi PN, Mbah HA, Burda S, Williams C, Gorny MK, Nadas A, Zolla-Pazner S. 2000.
567 Conserved and exposed epitopes on intact, native, primary human immunodeficiency virus
568 type 1 virions of group M. J Virol 74:7096-107.

569 42. Pinter A, Honnen WJ, He Y, Gorny MK, Zolla-Pazner S, Kayman SC. 2004. The V1/V2
570 domain of gp120 is a global regulator of the sensitivity of primary human immunodeficiency
571 virus type 1 isolates to neutralization by antibodies commonly induced upon infection. J Virol
572 78:5205-15.

573 43. Gorny MK, Conley AJ, Karwowska S, Buchbinder A, Xu JY, Emini EA, Koenig S, Zolla-
574 Pazner S. 1992. Neutralization of diverse human immunodeficiency virus type 1 variants by
575 an anti-V3 human monoclonal antibody. J Virol 66:7538-42.

576 44. Gorny MK, Williams C, Volsky B, Revesz K, Wang XH, Burda S, Kimura T, Konings FA,
577 Nadas A, Anyangwe CA, Nyambi P, Krachmarov C, Pinter A, Zolla-Pazner S. 2006. Cross-
578 clade neutralizing activity of human anti-V3 monoclonal antibodies derived from the cells of
579 individuals infected with non-B clades of human immunodeficiency virus type 1. J Virol
580 80:6865-72.

581 45. Hioe CE, Wrin T, Seaman MS, Yu X, Wood B, Self S, Williams C, Gorny MK, Zolla-Pazner
582 S. 2010. Anti-V3 monoclonal antibodies display broad neutralizing activities against multiple
583 HIV-1 subtypes. PLoS One 5:e10254.

584 46. Gigler A, Dorsch S, Hemauer A, Williams C, Kim S, Young NS, Zolla-Pazner S, Wolf H,
585 Gorny MK, Modrow S. 1999. Generation of neutralizing human monoclonal antibodies
586 against parvovirus B19 proteins. J Virol 73:1974-9.

587 47. Bradley KA, Mogridge J, Mourez M, Collier RJ, Young JA. 2001. Identification of the
588 cellular receptor for anthrax toxin. Nature 414:225-9.

589 48. Courtney CR, Agyingi L, Fokou A, Christie S, Asaah B, Meli J, Ngai J, Hewlett I, Nyambi
590 PN. 2016. Monitoring HIV-1 Group M Subtypes in Yaounde, Cameroon Reveals Broad
591 Genetic Diversity and a Novel CRF02_AG/F2 Infection. AIDS Res Hum Retroviruses
592 32:381-5.

593 49. Upadhyay C, Feyznezhad R, Yang W, Zhang H, Zolla-Pazner S, Hioe CE. 2018. Alterations
594 of HIV-1 envelope phenotype and antibody-mediated neutralization by signal peptide
595 mutations. PLoS Pathog 14:e1006812.

596 50. Rossio JL, Esser MT, Suryanarayana K, Schneider DK, Bess JW, Jr., Vasquez GM, Wiltrout
597 TA, Chertova E, Grimes MK, Sattentau Q, Arthur LO, Henderson LE, Lifson JD. 1998.
598 Inactivation of human immunodeficiency virus type 1 infectivity with preservation of
599 conformational and functional integrity of virion surface proteins. J Virol 72:7992-8001.

600 51. Stieh DJ, King DF, Klein K, Aldon Y, McKay PF, Shattock RJ. 2015. Discrete partitioning of
601 HIV-1 Env forms revealed by viral capture. Retrovirology 12:81.

602 52. Weiss S, Itri V, Pan R, Jiang X, Luo CC, Morris L, Malherbe DC, Barnette P, Alexander J,
603 Kong XP, Haigwood NL, Hessell AJ, Duerr R, Zolla-Pazner S. 2022. Differential V2-directed
604 antibody responses in non-human primates infected with SHIVs or immunized with diverse
605 HIV vaccines. Nat Commun 13:903.

606 53. Haynes BF, Gilbert PB, McElrath MJ, Zolla-Pazner S, Tomaras GD, Alam SM, Evans DT,
607 Montefiori DC, Karnasuta C, Sutthent R, Liao HX, DeVico AL, Lewis GK, Williams C,
608 Pinter A, Fong Y, Janes H, DeCamp A, Huang Y, Rao M, Billings E, Karasavvas N, Robb
609 ML, Ngauy V, de Souza MS, Paris R, Ferrari G, Bailer RT, Soderberg KA, Andrews C,
610 Berman PW, Frahm N, De Rosa SC, Alpert MD, Yates NL, Shen X, Koup RA, Pitisuttithum
611 P, Kaewkungwal J, Nitayaphan S, Rerks-Ngarm S, Michael NL, Kim JH. 2012. Immune-
612 correlates analysis of an HIV-1 vaccine efficacy trial. N Engl J Med 366:1275-86.

613 54. Mkhize NN, Durgiah R, Ashley V, Archary D, Garrett NJ, Karim QA, Karim SS, Moore PL,
614 Yates N, Passmore JA, Tomaras GD, Morris L. 2016. Broadly neutralizing antibody
615 specificities detected in the genital tract of HIV-1 infected women. AIDS 30:1005-14.

616 55. Yates NL, deCamp AC, Korber BT, Liao HX, Irene C, Pinter A, Peacock J, Harris LJ, Sawant
617 S, Hraber P, Shen X, Rerks-Ngarm S, Pitisuttithum P, Nitayapan S, Berman PW, Robb ML,
618 Pantaleo G, Zolla-Pazner S, Haynes BF, ..., Tomaras GD. 2018. HIV-1 Envelope
619 Glycoproteins from Diverse Clades Differentiate Antibody Responses and Durability among
620 Vaccinees. J Virol 92.

621 56. Rao PG, Lambert GS, Upadhyay C. 2023. Broadly neutralizing antibody epitopes on HIV-1
622 particles are exposed after virus interaction with host cells. J Virol 97:e0071023.

623 57. Lund J, Winter G, Jones PT, Pound JD, Tanaka T, Walker MR, Artymiuk PJ, Arata Y, Burton
624 DR, Jefferis R, et al. 1991. Human Fc gamma RI and Fc gamma RII interact with distinct but
625 overlapping sites on human IgG. J Immunol 147:2657-62.

626 58. Wilkinson I, Anderson S, Fry J, Julien LA, Neville D, Qureshi O, Watts G, Hale G. 2021. Fc-
627 engineered antibodies with immune effector functions completely abolished. PLoS One
628 16:e0260954.

629 59. Schlothauer T, Herter S, Koller CF, Grau-Richards S, Steinhart V, Spick C, Kubbies M, Klein
630 C, Umana P, Mossner E. 2016. Novel human IgG1 and IgG4 Fc-engineered antibodies with
631 completely abolished immune effector functions. Protein Eng Des Sel 29:457-466.

632 60. Lubeck MD, Steplewski Z, Baglia F, Klein MH, Dorrington KJ, Koprowski H. 1985. The
633 interaction of murine IgG subclass proteins with human monocyte Fc receptors. J Immunol
634 135:1299-304.

635 61. Temming AR, Bentlage AEH, de Taeye SW, Bosman GP, Lissenberg-Thunnissen SN,
636 Derksen NIL, Brasser G, Mok JY, van Esch WJE, Howie HL, Zimring JC, Vidarsson G.
637 2020. Cross-reactivity of mouse IgG subclasses to human Fc gamma receptors: Antibody
638 deglycosylation only eliminates IgG2b binding. Mol Immunol 127:79-86.

639 62. Zolla-Pazner S, Cohen SS, Boyd D, Kong XP, Seaman M, Nussenzweig M, Klein F,
640 Overbaugh J, Totrov M. 2016. Structure/Function Studies Involving the V3 Region of the
641 HIV-1 Envelope Delineate Multiple Factors That Affect Neutralization Sensitivity. J Virol
642 90:636-49.

643 63. Liu L, Cimbro R, Lusso P, Berger EA. 2011. Intraprotomer masking of third variable loop
644 (V3) epitopes by the first and second variable loops (V1V2) within the native HIV-1 envelope
645 glycoprotein trimer. Proc Natl Acad Sci U S A 108:20148-53.

646 64. Zolla-Pazner S, Cardozo T. 2010. Structure-function relationships of HIV-1 envelope
647 sequence-variable regions refocus vaccine design. Nat Rev Immunol 10:527-35.

648 65. Zohar T, Alter G. 2020. Dissecting antibody-mediated protection against SARS-CoV-2. Nat
649 Rev Immunol 20:392-394.

650

Figure 1.

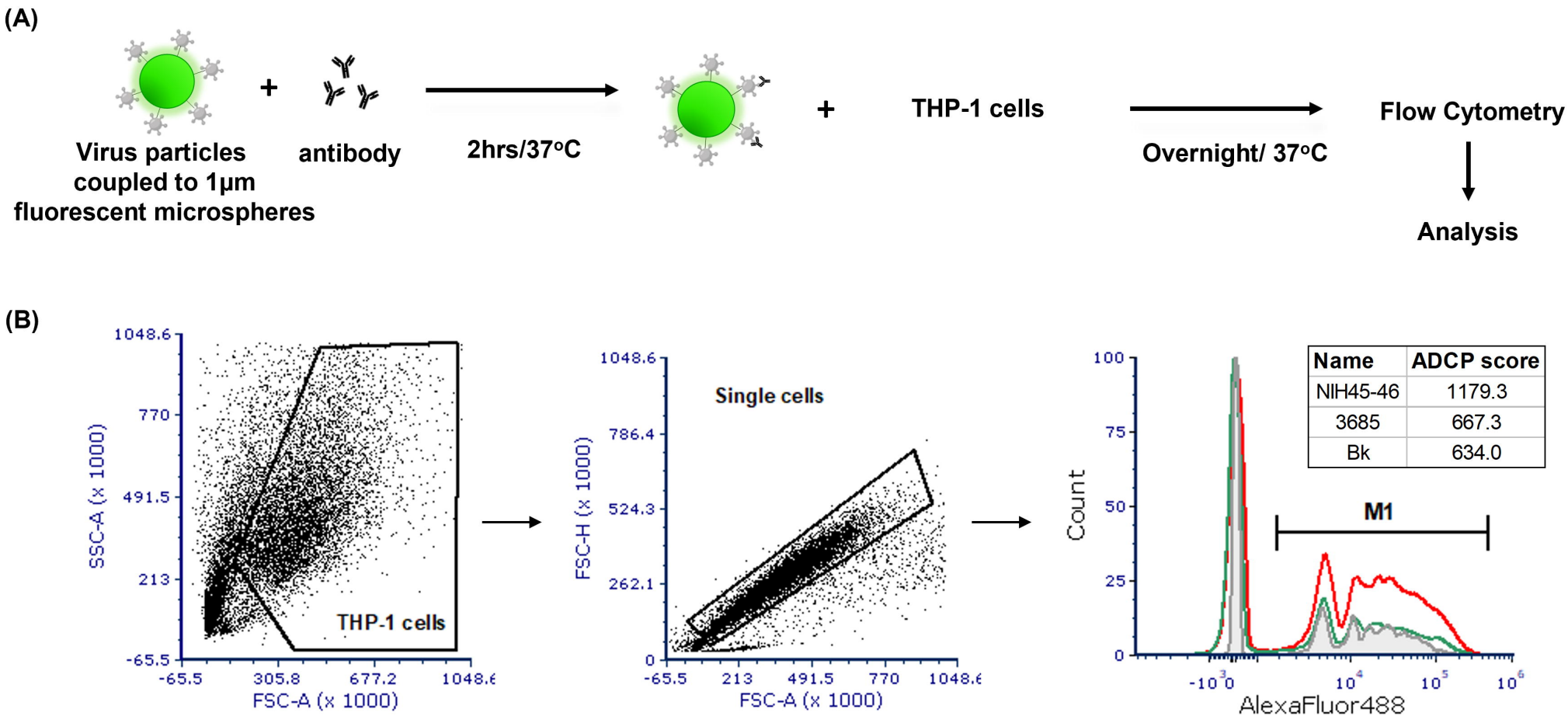
(A)
Virus particles coupled to 1µm fluorescent microspheres
+
antibody
2hrs/37°C
+
THP-1 cells
Overnight/ 37°C
Flow Cytometry
Analysis
(B)
SSC-A (x 1000)
FSC-A (x 1000)
THP-1 cells
FSC-H (x 1000)
Single cells
Count
AlexaFluor488
M1
Name | ADCP score
NIH45-46 | 1179.3
3685 | 667.3
Bk | 634.0

Figure 2.

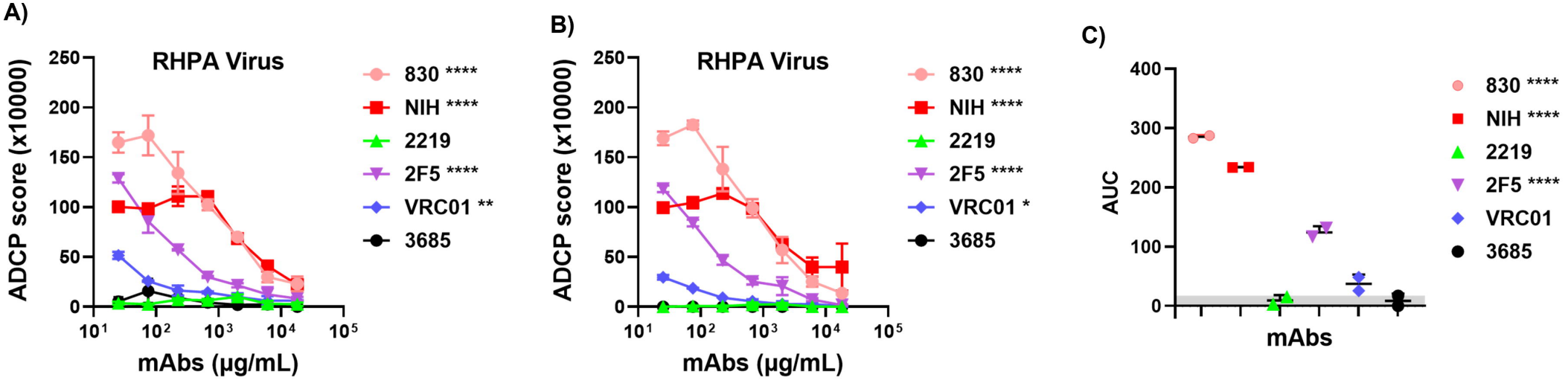
A)
RHPA Virus
ADCP score (x10000)
mAbs (µg/mL)
830 ****
NIH ****
2219
2F5 ****
VRC01 **
3685
B)
RHPA Virus
ADCP score (x10000)
mAbs (µg/mL)
830 ****
NIH ****
2219
2F5 ****
VRC01 *
3685
C)
AUC
mAbs
830 ****
NIH ****
2219
2F5 ****
VRC01
3685

Figure 3.

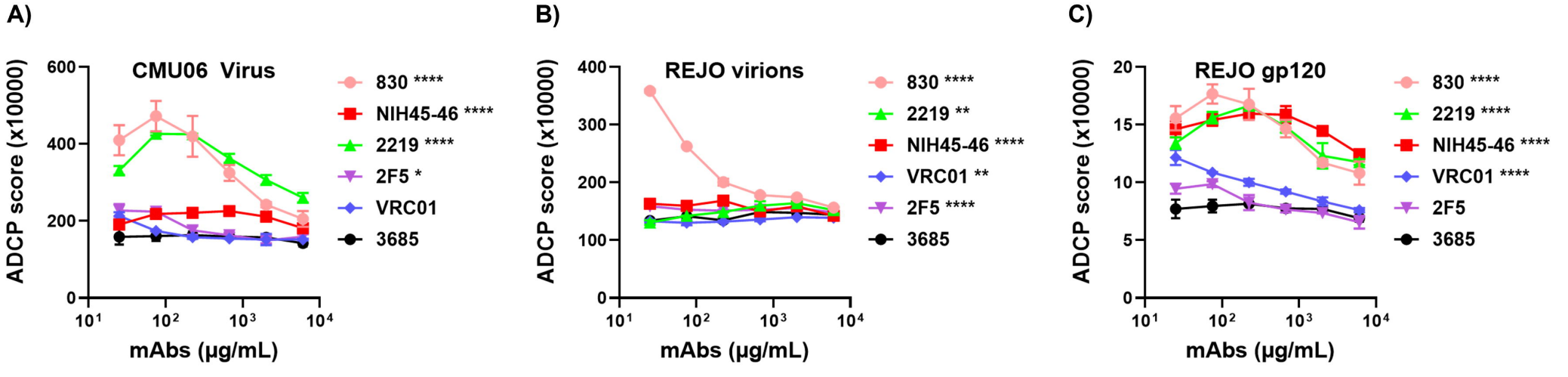
A)
CMU06 Virus
ADCP score (x10000)
mAbs (µg/mL)
830 ****
NIH45-46 ****
2219 ****
2F5 *
VRC01
3685
B)
REJO virions
ADCP score (x10000)
mAbs (µg/mL)
830 ****
2219 **
NIH45-46 ****
VRC01 **
2F5 ****
3685
C)
REJO gp120
ADCP score (x10000)
mAbs (µg/mL)
830 ****
2219 ****
NIH45-46 ****
VRC01 ****
2F5
3685

Figure 4.

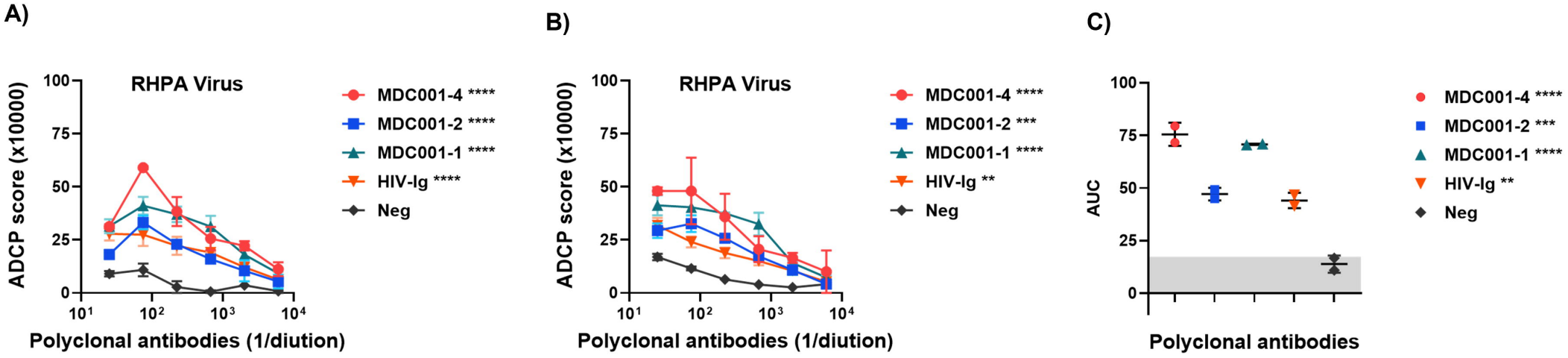
A)
RHPA Virus
ADCP score (x10000)
100
75
50
25
0
10^1
10^2
10^3
10^4
Polyclonal antibodies (1/diution)
MDC001-4 ****
MDC001-2 ****
MDC001-1 ****
HIV-Ig ****
Neg
B)
RHPA Virus
ADCP score (x10000)
100
75
50
25
0
10^1
10^2
10^3
10^4
Polyclonal antibodies (1/diution)
MDC001-4 ****
MDC001-2 ***
MDC001-1 ****
HIV-Ig **
Neg
C)
AUC
100
75
50
25
0
Polyclonal antibodies
MDC001-4 ****
MDC001-2 ***
MDC001-1 ****
HIV-Ig **
Neg

Figure 5.

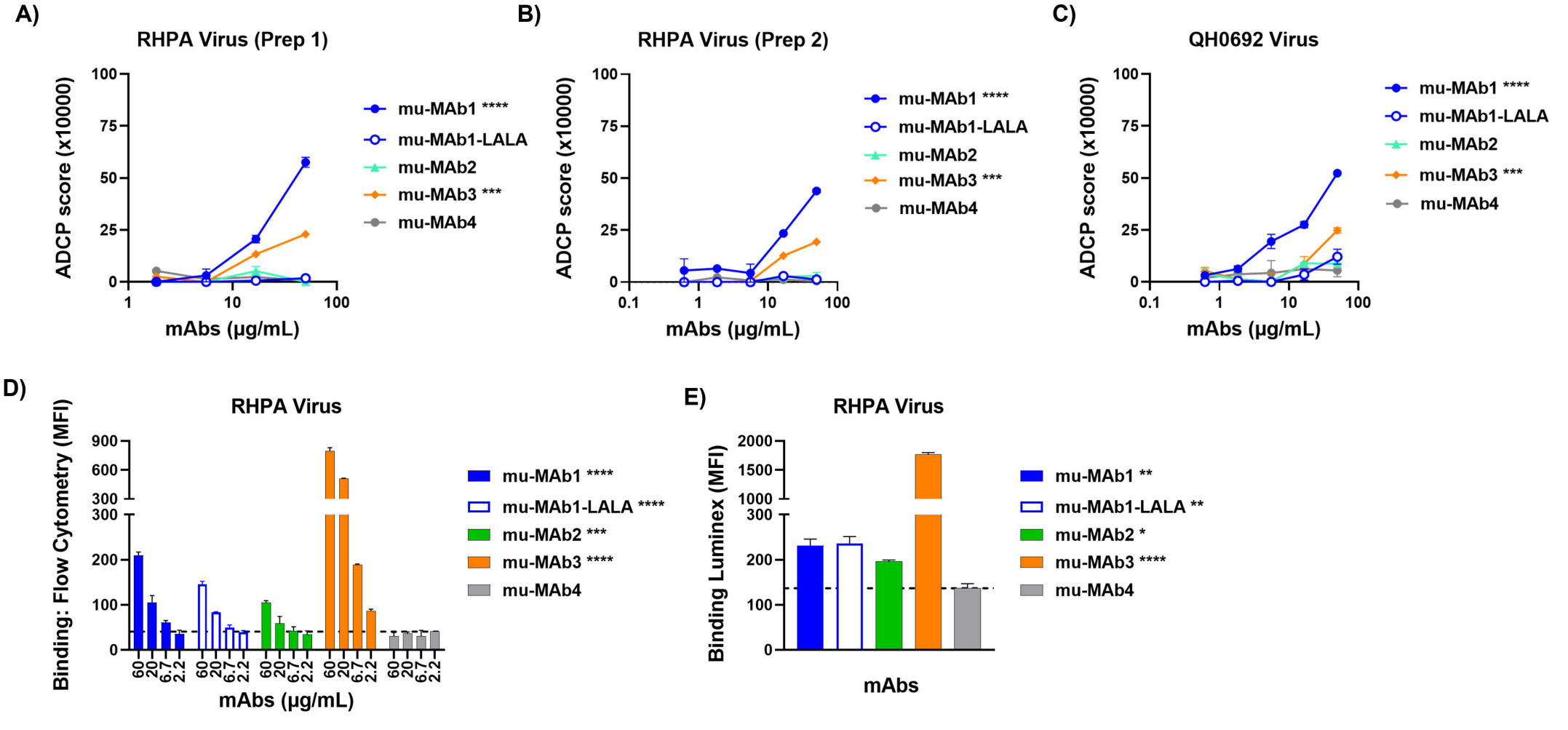
A)
RHPA Virus (Prep 1)
ADCP score (x10000)
mAbs (µg/mL)
mu-MAb1 ****
mu-MAb1-LALA
mu-MAb2
mu-MAb3 ***
mu-MAb4
B)
RHPA Virus (Prep 2)
ADCP score (x10000)
mAbs (µg/mL)
mu-MAb1 ****
mu-MAb1-LALA
mu-MAb2
mu-MAb3 ***
mu-MAb4
C)
QH0692 Virus
ADCP score (x10000)
mAbs (µg/mL)
mu-MAb1 ****
mu-MAb1-LALA
mu-MAb2
mu-MAb3 ***
mu-MAb4
D)
RHPA Virus
Binding: Flow Cytometry (MFI)
mAbs (µg/mL)
mu-MAb1 ****
mu-MAb1-LALA ****
mu-MAb2 ***
mu-MAb3 ****
mu-MAb4
E)
RHPA Virus
Binding Luminex (MFI)
mAbs
mu-MAb1 **
mu-MAb1-LALA **
mu-MAb2 *
mu-MAb3 ****
mu-MAb4

Figure 6.

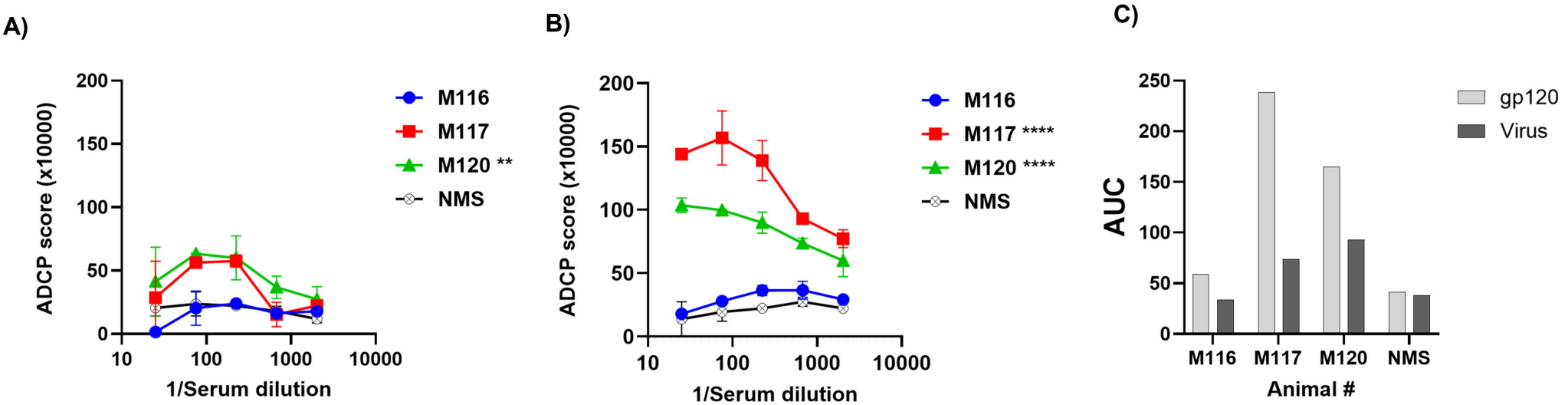
A)
ADCP score (x10000)
200
150
100
50
0
10
100
1000
10000
1/Serum dilution
M116
M117
M120 **
NMS
B)
ADCP score (x10000)
200
150
100
50
0
10
100
1000
10000
1/Serum dilution
M116
M117 ****
M120 ****
NMS
C)
AUC
250
200
150
100
50
0
M116
M117
M120
NMS
Animal #
gp120
Virus